The Effect of Pore Size on Cell Adhesion in Collagen-GAG Scaffolds

F. J. O'Brien[1,4], B. A. Harley[2], I.V. Yannas[2, 3], L. J. Gibson[1]

Department of Materials Science and Engineering[1]
Department of Mechanical Engineering[2]
Division of Biological Engineering[3]
Massachusetts Institute of Technology, Cambridge, MA 02139

Department of Anatomy, Royal College of Surgeons in Ireland,
St. Stephen's Green, Dublin 2, Ireland[4]

Corresponding Author:

Prof. L.J. Gibson
Department of Materials Science and Engineering
Massachusetts Institute of Technology
77 Massachusetts Avenue, Rm. 8-135
Cambridge, MA 02139
Email: ljgibson@mit.edu
Voice: (617) 253-7107
Fax: (617) 258-6275

Abstract

The biological activity of scaffolds used in tissue engineering applications hypothetically depends on the density of available ligands. Ligand density is characterized by the composition of the scaffold, which defines the surface density of ligands, and by the specific surface area of the scaffold, which defines the total surface of the structure exposed to the cells. It has been previously shown that collagen-glycosaminoglycan scaffolds used in skin regeneration studies were inactive when the average pore diameter was either lower than 20 μm or higher than 120 μm[1]. It has been hypothesized that while the lower limit in pore diameter is set by the requirement for pores large enough for cell migration inside the scaffold, the upper limit reflects the requirement for a sufficient density of ligands to which cells can bind. A test of this hypothesis was made in this study. Collagen-GAG (CG) scaffolds were manufactured using a lyophilization technique, varying the final temperature of freezing to produce a homologous series of four scaffold types with a constant composition and solid volume fraction (0.005) but with four different pore sizes corresponding to four levels of the specific surface. MC3T3-E1 mouse clonal osteogenic cells were seeded onto the four scaffold types and maintained in culture for 24 and 48 hours; at the end-point, the remaining viable cells were counted to determine the percent cell attachment. It was observed that variation in specific surface in the four scaffolds resulted in a significant difference in cell attachment at both 24 and 48 hours; however, there was no significant change in cell attachment between 24 and 48 hours for any group. The fraction of cells attached to the CG scaffold decreased with increasing average pore diameter, and increased linearly with specific surface area calculated using a cellular solids model of the pore structure (R^2 = 0.95, 0.91

at 24 and 48 hours, respectively). These results show that an increase in ligand density leads to a larger fraction of the seeded cells attaching onto the scaffold, consistent with the hypothesis for scaffold bioactivity described above.

Keywords: collagen, scaffold, microstructure, cell adhesion, ligands

Running Head: Cell Adhesion in Collagen-GAG Scaffolds

INTRODUCTION

Porous, three-dimensional scaffolds have been used extensively as a biomaterial in the field of tissue engineering for both *in vitro* study of cell-scaffold interactions and tissue synthesis and for *in vivo* study of induced tissue and organ regeneration. In both *in vivo* and *in vitro* models, the three-dimensional scaffolds serve as an analog of the extracellular matrix, acting as a physical support structure that affects cellular processes such as migration, contraction, and division. Scaffolds made from collagen have been commonly used in a variety of tissue engineering applications due to a number of beneficial properties; collagen is a significant consitituent of the extracellular matrix, it has beneficial antigenic, hemostatic, and mechanical properties, and it promotes cellular binding. In designing bioactive scaffolds for *in vivo* regeneration experiments, there are four critical properties to consider: a collagen fiber structure where the periodic banding has been selectively abolished to prevent platelet aggregation on the fibers; a chemical composition that incorporates ligands appropriate for the binding of cells specific to the area of study; an average pore diameter that is bounded within a lower and upper limit; a degradation rate that allows the scaffold to remain insoluble just for the duration of the regeneration process at the injured site[2, 3]. Focusing on the pore size requirement, the pores need to be large enough to allow cells to migrate into the structure, where they eventually become bound to the scaffold, but small enough to establish a sufficiently high specific surface for a minimal ligand density to allow efficient binding of a critical amount of cells to the scaffold[2]. In order to properly investigate the effect of the scaffold structure on cell behavior, it is first necessary to develop a process to fabricate scaffolds with uniform but variable pore structures.

While cell attachment to the scaffold appears to play a critical role during *in vivo* synthesis of organs (induced regeneration), it has also been used as a measure of cell viability for *in vitro* studies[4-6]. The scaffold pore structure has been observed to significantly affect cell binding and migration *in vitro* and influence the rate and depth of cellular ingrowth into the scaffold *in vitro* and *in vivo*[7, 8]. Additionally, cell adhesion and activity has been observed to vary considerably depending on the cell type, as well as the scaffolds composition and pore size[9-11]. In porous silicon nitride scaffolds, endothelial cells bind only to pores smaller than 80 μm while fibroblasts preferentially bind to larger pores (>90 μm). In PLLA scaffolds, vascular smooth muscle cells preferentially bind to one range of pore sizes (63 - 150 μm) while fibroblasts bind to a wider range (38 - 150 μm)[12, 13]. A number of cell types exhibit preferences to binding in scaffolds with pore sizes considerably larger than the characteristic cell size, often utilizing a characteristic bridging mechanism where adjacent cells act as support structures to assist bridging large pores; examples include fibrovascular tissue ingrowth into PLLA scaffolds, osteoblast adhesion to polylactide-co-glycolide (PLAGA) scaffolds, and rat marrow cells binding to PEOT/PBT scaffolds[7, 14, 15]. Additionally, the mean pore size of scaffolds has also been shown to significantly influence cell morphology and phenotypic expression[16-18]. Based upon the scaffold design rules and a series of experiments, it has been assumed that there is an optimal pore size for each specific tissue engineering application.

Scaffolds manufactured from a copolymer of collagen and glycosaminoglycan (CG copolymers) possess a number of useful qualities for use as tissue engineering constructs: they can be sterilized by both dry heat and chemical treatments, they have degradation rates that can be adjusted within a wide range, and they can be fabricated from a number of macromolecular constituents with a variety of pore structures. This study utilized a porous, type I collagen-glycosaminoglycan (CG) scaffold; distinct versions of this scaffold have induced partial regeneration of skin in burn patients and in patients undergoing plastic and reconstructive surgery, have induced regeneration of the conjunctiva, have greatly enhanced peripheral nerve regeneration across long (>25 mm) gaps in the transected rat sciatic nerve[1, 2], and have been studied *in vitro* in a wide variety of cellular migration and contraction studies[1, 2, 17, 19, 20].

The CG scaffolds used in this experiment are fabricated using a freeze-drying (lyophilization) process[2] where a suspension of collagen and glycosaminoglycans is solidified (frozen) leaving the CG co-precipitate localized between the growing ice crystals during the freezing process, forming a continuous, interpenetrating network of ice and the coprecipitate[21, 22]. Sublimation of the ice crystals forms the highly porous scaffold structure similar to a sponge. The pore volume fraction and the size of the pores can be controlled by the volume fraction of the precipitate in the suspension and by the underlying freezing processes; typical pore volume fractions of these scaffolds are above 99%. The formation of individual ice crystals within the CG suspension is influenced by the rate of nucleation of ice crystals and the rate of heat and protein diffusion, processes primarily controlled by the final temperature of freezing (T_f) and the heat transfer

processes associated with freezing. The rate of nucleation and diffusion are mediated by the difference between the temperature of freezing and the actual temperature of the material during the freezing process (undercooling)[21] where a larger undercooling increases the rate of ice crystal nucleation and decreases the rate of heat and protein diffusion relative to the point of nucleation[21, 22]. With larger undercooling temperatures, smaller ice crystals are formed, resulting in a CG scaffold with a smaller average pore diameter[23, 24].

A constant cooling rate technique has been developed in this laboratory to fabricate CG scaffolds with a homogeneous pore structure exhibiting equiaxed pores by controlling the rate at which the suspension freezes during synthesis[25]. During the fabrication process, the temperature of the freeze-dryer was cooled at a constant rate from room temperature to the final temperature of freezing (T_f) over an interval of critical duration. This fabrication technique has significantly improved the structural uniformity of the CG scaffolds: the CG scaffold has significantly more homogeneous structure with a small variation in mean pore size throughout the scaffold (T_f = -40ºC; Mean Dia.: 95.9 μm, Coefficient of Variance 0.128). Additionally, the pores produced using the constant cooling rate technique are characterized by pore channel axes that are much more randomly oriented than scaffolds fabricated using the earlier quenching technique[25]. The constant cooling technique had not been applied to fabricate uniform CG scaffolds with different pore sizes, a requirement for any attempt to probe the effects of pore size on cell behavior.

The objective of this study was to determine the effect of the average pore diameter of the collagen-GAG scaffold on cell attachment using MC3T3 cells. The MC3T3 cell line was used to study the viability of an osteoblast-like cell in a collagen-GAG scaffold for orthopedic applications[26]. The primary goal was to modify the previously reported temperature ramping technique to produce homogeneous scaffolds with variable pore sizes. The constant cooling rate technique for was modified to fabricate scaffolds at a series of final temperatures of freezing from -10ºC to -40ºC. The pore size and structure of these new scaffolds were assessed and the attachment behavior of cells on each of these scaffolds was measured to determine whether both the mean pore size and the specific surface area of collagen-GAG scaffolds influence cell adhesion.

MATERIALS AND METHODS

Preparation of collagen-glycosaminoglycan co-polymer suspension

The CG scaffolds were fabricated from a CG suspension using a lyophilization method that utilizes a constant cooling rate freezing step to produce scaffolds with an equiaxed pore structure[1, 25]. The CG suspension was produced by combining microfibrillar, type I collagen isolated from bovine tendon (Integra LifeSciences, Plainsboro, NJ) and chondroitin-6-sulfate isolated from shark cartilage (Sigma-Aldrich Chemical Co., St. Louis, MO) in a solution of acetic acid where the final suspension contained 0.5 wt% collagen and 0.05 wt% chondroitin-6-sulfate. The collagen, chondroitin-6-sulfate, and 0.05M acetic acid (pH 3.2) were mixed at 15,000 rpm in an overhead blender (IKA Works, Inc., Wilmington, NC). The temperature of the suspension was maintained at 4^{o}C throughout the entire mixing process by a cooling system (Brinkman, Westbury, CT) in

order to prevent denaturation of the collagen fibers due to inadvertent heating of the solution during mixing. After mixing, the CG suspension was degassed under vacuum (50 mTorr) for 60 minutes to remove air bubbles introduced by the mixing process and was then stored at 4ºC until use. Immediately prior to use, the volume of suspension was degassed for a second time, allowing the suspension to reach room temperature.

Fabrication of CG scaffold with different pore sizes

Prior to sublimation, the CG suspension was frozen using the constant cooling rate technique that has been previously identified as a process to fabricate scaffolds with an equiaxed pore structure[25]. The degassed CG slurry was poured slowly into a 304 stainless steel tray (12.7 mm x 12.7 mm) (VirTis, Gardiner, NY) that was then placed into the chamber of a freeze-dryer (VirTis) for lyophilization. Briefly, the CG suspension in the tray was placed onto the shelf in the freeze-dryer chamber that was at room temperature (20ºC). The temperature of the freeze-dryer shelf and chamber was then cooled at a constant rate to the final temperature of freezing (T_f); the shelf/chamber temperature was then held constant for 60 minutes to complete the freezing process. Final freezing temperatures of -10^{o}C, -20^{o}C, -30^{o}C and -40^{o}C were used to attempt to produce porous scaffolds of four different mean pore sizes[27, 28]. The ice phase was then sublimated under a vacuum (below 100 mTorr) at 0^{o}C for a period of 17 hours to produce the porous CG scaffolds.

The temperature of the CG suspension and the freeze-dryer shelf during the freezing process was monitored at one minute intervals at four locations in the suspension using a

two-channel microprocessor thermocouple (HH22, Omega Engineering, Stamford, CT) as has been previously described[25]. The average freezing rate of the suspension in ºC/min was determined as the average rate of freezing from the starting temperature of the suspension to a lower limit. The lower limit was set to be 5ºC greater than the final temperature of freezing, and was used in this calculation because below that temperature, the temperature of the suspension and the freeze-dryer shelf tended to asymptotically approach the final temperature of freezing, and could not be modeled linearly.

CG scaffold crosslinking

All CG scaffolds manufactured in this study were cross-linked via a dehydrothermal process after freeze-drying to stiffen the collagen network. Cross-linking was carried out in a vacuum oven (Fisher IsoTemp 201, Fisher Scientific, Boston, MA) at a temperature of 105^{o}C under a vacuum of 50 mTorr for 24 hours[1, 25]. This process introduced covalent cross-links between the polypeptide chains of the collagen fibers without denaturing the collagen into gelatin[29].

Analysis of pore structure

The pore structure analysis method has been described previously[25]. To determine the average pore size of each scaffold, pairs of samples were removed from five fixed locations throughout each sheet of the CG scaffold. At each of the five locations in each CG sheet, samples were taken from the longitudinal plane (10 x 10 x 3 mm thick square section from the plane of the scaffold) and in an adjacent region from the transverse plane (10 x 5 x 3 mm thick rectangular section from the plane of the scaffold). Each sample

was embedded in glycolmethacrylate and serially sectioned on a Leica RM2165 microtome (Mannheim, Germany) at a 5 μm thickness. The sections were stained using aniline blue and observed on an optical microscope (Nikon Optiphot, Japan) at 4x magnification. Images were digitized from each longitudinal and transverse section using a CCD color video camera (Optronics Engineering, Inc., Goleta CA). The digitized images were then analyzed using a linear intercept program in Scion Image™ software (Scion Corp., Frederick, MD) to determine the average pore size of the pore field in each cross-sectional image. Briefly, the program calculated the number of times that a series of parallel lines drawn across the image intercepted a pore wall. This process was repeated with the series of parallel lines rotated by 5° increments around the section and the mean intercept length, or average distance between pore walls was reported. The linear intercept program utilized the distance and angle measurements to construct a best-fit ellipse representing an average pore cross-section for the regions analyzed. The mean pore diameter at each position within the scaffold was calculated from the average of the analysis results from the longitudinal and transverse planes at that location. The best-fit ellipses calculated for the adjoining transverse and longitudinal sections were used to construct a best-fit ellipsoid. Averaging the results from all analyzed locations throughout the scaffold generated the mean pore diameter value for each scaffold produced at the four freezing temperatures. Previous results indicated that scaffold produced using the constant cooling rate techniques had an equiaxed pore structure[25], and the average pore size of scaffolds in this study was determined by averaging measurements from both the longitudinal and transverse sections.

Relationship between specific surface area and pore size

The biological activity of a scaffold depends on a number of biochemical and mechanical parameters; in this study, the surface area per unit volume (SA/V) or specific surface area of the scaffold was studied. For a open cell foam with an interconnected pore structure modeled using a polyhedral unit cell, the specific surface area can be related to the pore size and the relative density (the density of the porous material relative to that of the solid it is made from)[30]. We have used a tetrakaidecahedral unit cell (a fourteen-sided polyhedron that packs to fill space) to model the geometry of the porous scaffold. The pore structure of a variety of low-density foams has been observed to have three distinct features[31]: there are an average of approximately 14 faces per cell, an average of 5.1 edges per face, and the vertices are nearly tetrahedral. These morphological features come as a result of a minimization of the total surface area of the closed cells. The tetrakaidecahredon is a polyhedron that packs to fill space, approximates the structural features observed through experiment, nearly satisfies the minimum surface energy condition, and is often used for modeling low-density foams[30, 32]. In addition, for the tetrakaidecahedral unit cell, the value of the dimensionless measure of total edge length per (unit volume)$^{1/3}$ for the unit cell is nearly identical to that observed for many random cellular structures[33], suggesting that the tetrakaidecahedral unit cell gives a good representation of the total edge length and can be used to model the specific surface area of random cellular structures such as the porous, CG scaffold. For an open-cell tetrakaidecahedron with edges of circular cross-section, the specific surface area is:

$$\frac{SA}{V} = \frac{3.65}{l}\left(\frac{\rho^*}{\rho_s}\right)^{1/2} \qquad (1)$$

In this relation, l is the edge length of the tetrakaidecahedron, ρ^* is its density, and ρ_s is the density of the solid from which it is made. The relative density (ρ^*/ρ_s) of the collagen-GAG scaffolds was determined by measuring the density of entire sheets of CG scaffold, and was measured to be constant, with a value of 0.5%. The specific surface area equation (1) can then be simplified:

$$\frac{SA}{V} = \frac{0.258}{l} \tag{2}$$

To calculate the mean spacing (equivalent to diameter) between opposite sides of this structure, we assume that the internal volume is similar to that of a sphere of diameter d. Using this assumption the pore diameter can be calculated by:

$$d = 2.78l \tag{3}$$

Additionally, the volume of an individual tetrakaidecahedron is ($11.31l^3$)[34]. From this calculation, we estimate that the specific surface area of the scaffolds is related to the pore diameter by:

$$\frac{SA}{V} = \frac{0.718}{d} \tag{4}$$

Cell adhesion study

Four sets of scaffolds, each set having a different mean pore diameter, were fabricated using the technique described. Full thickness (approximately 3 mm thick) samples, 30 mm x 22 mm in size, were cut from the fully processed CG scaffold for the cell adhesion experiments described below.

Cell Culture

MC3T3-E1 mouse clonal osteogenic cells were maintained in α-MEM supplemented with L-glutamine, 10% fetal bovine serum (FBS; Intergen, Purchase, NY, USA), penicillin (100 IU/ml; Sigma), and streptomycin (100 mg/ml; Sigma). A suspension of 2^{nd} through 7^{th} passage cells were removed from the culture flask with trypsin-EDTA (Sigma, St. Louis, MO) to harvest cells for use in seeding the CG scaffolds. Viable cell number was determined prior to seeding by live-cell staining using 0.4% Trypan Blue (Invitrogen Co., Chicago, IL) and counting viable cells with a standard hemacytometer (Bright-Line, Hausser Scientific, Horsham, PA)[20].

Prior to seeding, the scaffold samples were placed into individual wells of a 6-well tissue culture plate (Nalge Nunc International, Naperville, IL). Each well was pre-coated with agarose gel (J.T. Baker, Philipsburg, NJ) to prevent cells from migrating out of the scaffolds and on to the tissue culture plate. The CG scaffold was seeded on both sides with 3×10^6 cells in a manner that has previously been described[19, 20]. One milliliter of the MC3T3-E1 cell suspension (3×10^6 cells/ml) was pipetted onto the surface of the dry scaffold. The scaffold was then returned to the incubator for 10 minutes to allow for

initial cell attachment; the seeded scaffold was then turned over and an additional 1 ml of the cell suspension was pipetted onto the reverse surface of the scaffold. The wells were then filled with 2 ml of the supplemented (L-glutamine, FBS, penicillin, streptomycin) α-MEM media and placed into a cell culture incubator and maintained in an environment of 37ºC with 5.0% CO_2.

Cell counting

Following each adhesion experiment, the seeded scaffold sample was removed from the tissue culture plate. Each sample was rinsed with Dulbecco's phosphate buffered saline (DPBS) (Gibco, Grand Island, NY) at 37°C to remove unattached cells and was then placed in a 2.0 U/ml solution of dispase (Gibco, Grand Island, NY) for 30 minutes to digest the scaffold[19, 20]. The cells were then stained with 0.4% Trypan Blue and the number of attached cells was counted using a hemacytometer.

Statistical analysis

One-way analysis of variance (ANOVA) and pairwise multiple comparison procedures (Dunn's Method) were used to compare groups of data. Paired t-tests were performed to compare individual sets of data in order to determine statistical significance (between 24 and 48 hour groups within the same scaffold). Error is reported in figures as the standard deviation (StDev), the standard error of the mean (SEM = $StDev/n^{1/2}$), or as the coefficient of variance (CV = StDev/Mean). A probability value of 95% ($p < 0.05$) was used to determine significance.

RESULTS

Rate of freezing of CG suspension

Figure 1 shows the average temperature of the freeze-dryer shelf as well as the average temperature of the CG suspension during freezing for the four freezing protocols (T_f = -10, -20, -30, -40°C). The freezing profile of the freeze-dryer shelf follows the same initial curve for all four freezing protocols. While the rate of freezing of the CG suspension has previously been reported (0.9ºC/min)[25], the freezing profile of the freeze-dryer shelf will be reported here. The CG suspension was exposed to the same freezing profile (constant cooling rate of approximately 1.4°C/min) for all freezing protocols to the point where the final temperature of freezing was reached; at that point, the undercooling was maintained for the remainder of the freezing profile (**Fig. 1a**). The freezing curves of the CG suspension remained similar for the four freezing protocols until the point of maximal supercooling was reached (between -5.3°C and -8.2°C). After reaching the point of maximal supercooling, the CG suspension showed qualitatively similar freezing curves as each suspension asymptotically approached the final temperature of freezing. As expected, the CG suspension approached the final temperature of freezing more rapidly when exposed to greater undercooling (lower T_f) (**Fig. 1b**).

Effect of final freezing temperature on pore size

All the collagen-GAG scaffolds produced appeared to have a homogeneous pore structure with no obvious areas of non-uniformity in pore size or structure in individual scaffolds when viewed with the naked eye prior to histological examination. Such gross examination has previously sufficed to identify areas of heterogeneity and homogeneity in scaffolds of this type. **Figure 2** shows the effect of freezing temperature on the mean

pore size in the scaffolds. Scaffolds fabricated at a final temperature of freezing of -40ºC, -30ºC, -20ºC and -10ºC were determined to have a mean pore size of 95.9 μm, 109.5 μm, 121.0 μm and 150.5 μm, respectively. One-way analysis of variance (ANOVA) showed the final temperature of freezing has a significant effect on the mean pore size ($p < 0.001$). Pos-hoc testing between each of the mean pore sizes of the four different scaffolds indicated that there was a significant difference in mean pore size between all groups ($p < 0.05$).

Figure 2 also shows the results of the detailed pore analysis of the four different CG scaffolds. The mean pore structure of each scaffold was determined in both the longitudinal and transverse (cross-sectional) planes of the scaffold in a manner previously described[25] in order to estimate the three-dimensional geometry of the pores. In scaffolds produced at freezing temperatures of -40ºC, -30ºC, -20ºC, no significant difference was found in intercept length between the two planes analyzed in the scaffold ($p > 0.05$). The coefficient of variance for scaffolds produced at freezing temperatures of -40ºC, -30ºC, and -20ºC was 0.128, 0.167 and 0.186, respectively, indicating an equiaxed pore structure as has been previously observed when freezing to -40ºC. However, a significant difference in mean pore size of the longitudinal (163.9 ± 31.6 μm) and transverse (130.4 ± 20.6 μm) planes ($p < 0.05$) was observed for CG scaffolds produced at a final temperature of freezing of -10°C. Consequently, scaffolds produced at this temperature, whilst having the largest pore diameter were also found to have the largest coefficient of variance (0.213). All four types of scaffolds had a consistent pore structure, with no significant variation in mean pore size, structure, or alignment at separate points

spatially within the scaffold ($p > 0.05$), suggesting that fabrication of a uniform pore structure throughout the scaffold.

Figure 3 shows a series of micrographs taken from scaffolds fabricated using different final freezing temperatures. The increase in mean pore size as a result of increasing the final freezing temperature is clearly evident in these images. Pores were observed to be largely equiaxed with no obvious local alignment of pore channel axes.

Cell adhesion study

Effect of pore size on adhesion

Figure 4 shows the percentage of MC3T3-E1 cells seeded onto the matrix which were attached to the four different scaffolds at both 24 and 48 hours post-seeding. One-way analysis of variance (ANOVA) indicated that mean pore diameter of the scaffolds had a significant effect on cell attachment after both 24 ($p < 0.01$) and 48 hours ($p < 0.001$). In the scaffolds with the smallest mean pore size (95.9 μm; T_f = -40ºC) over 40% of cells seeded attached to the scaffolds at both 24 and 48 hours compared to approximately 20% of cells that remained attached to the scaffolds with the largest mean pore size (150.5 μm; T_f = -10ºC). No significant difference in cell attachment was found between the intermediate scaffolds (mean pore size of 109.5 μm and 121.0 μm) with approximately 30% of cells (31.1% and 27.5% respectively) remaining attached after both the 24 hour and 48 groups ($p = 0.99$, $p = 0.89$ respectively).

Effect of seeding time on adhesion

Paired t-tests indicated that there was no statistical difference between the percentage of cells attached at 24 and 48 hours-post seeding for any of the four groups of scaffolds ($p > 0.05$).

Relationship between pore size and pore surface area

The specific surface area of the scaffold for each of the four different mean pore sizes was calculated using equation (4). The scaffold with the smallest mean pore size (95.9 μm; T_f = -40ºC) had the largest specific surface area of 0.00733 μm^{-1}, while the scaffold with the largest pore diameter (150.5 μm; T_f = -10ºC) had the smallest specific surface area of 0.00469 μm^{-1}. **Figure 5** shows a graph of percentage of seeded cells that remained attached to the scaffold plotted against specific surface area showing strong linear relationships (R^2 = 0.95, 0.91) between specific surface area (SA/V), calculated using equation (4), and the percent attached cells (PAC) at 24 hours and 48 hours post seeding, respectively. The linear regression equations were calculated to be:

$$PAC(24hrs) = 7207.9 \times (SA/V) - 12.916 \qquad R^2 = 0.95 \qquad (5)$$

$$PAC(48hrs) = 9522.0 \times (SA/V) - 28.999 \qquad R^2 = 0.91 \qquad (6)$$

DISCUSSION

Both the final freezing temperature and the heat transfer processes associated with freezing control the structure of CG scaffolds fabricated via a freeze-drying technique. The formation of individual ice crystals within a liquid medium is influenced by both the

nucleation of ice crystals and the rate of diffusion associated with the liquid, both of which are mediated by the final freezing temperature. Although the final temperature of freezing was varied in this study in order to manufacture CG scaffolds of varying pore size, a consistent freeze-dryer shelf cooling rate was maintained throughout (1.4°C/min). The four different final temperatures of freezing (-40ºC, -30ºC, -20ºC and -10ºC) produced four distinct scaffolds with different mean pore sizes (95.9 μm, 109.5 μm, 121.0 μm and 150.5 μm, respectively). Each scaffolds had a consistent pore structure and showed no obvious variation in mean pore size, structure, or alignment at separate points within the scaffold, indicating the homogeneity of the scaffolds produced.

For scaffolds produced at freezing temperatures of -40ºC, -30ºC and -20º, no significant variation in mean intercept length was found between the longitudinal and transverse planes showing that the pores formed in these scaffolds were uniform in shape as well as in size, i.e. scaffolds with an equiaxed pore structure were produced. However scaffolds produced at a freezing temperature of -10°C were found to have a significant variation in pore diameter between the longitudinal (163.9 ± 31.6 μm) and transverse (130.4 ± 20.6 μm) planes ($p > 0.05$). This suggests that at this higher freezing temperature, columnar ice crystals are formed rather than the more equiaxed and less elongated ice crystals that form at the lower temperatures of freezing. This result also parallels previous studies that have shown that the direction and speed of heat transfer during freezing influence the shape of ice crystals, where elongated ice crystals are formed when a predominant direction of heat transfer exists during the freezing process[21, 22, 24, 27].

The specific surface area available for cell binding determined using the tetrakaidecahedral model for the four scaffold variants, assumed to be proportional to the number of ligands available for binding, was found to be inversely proportional to the mean pore diameter (equation 4). Using the tetrakaidecahedral unit cell to model the random cellular structure of the CG scaffolds, the estimate of the specific surface area of the different scaffolds is remarkably consistent with the results from the cell attachment study, showing a linear relationship between percent cell attachment and specific surface area. The attached cell number increases linearly with specific surface area for data taken both at 24 hours ($R^2 = 0.95$) and at 48 hours ($R^2 = 0.91$) post-seeding.

No significant difference was observed in the percentage of cell attachment after 24 and 48 hours. This finding is consistent with the work of Freyman et al.[19] who found that**,** although there was a significant effect of time on fibroblast attachment in collagen-GAG scaffolds similar to those used in this study in the first hours post seeding, by 22 hours maximum attachment had been reached. The fraction of MC3T3-E1 cells attached to the collagen-GAG scaffold over the range of pore sizes studied decreases with increasing average pore diameter and increases linearly with specific surface area, consistent with the increase in ligand binding site density.

CONCLUSIONS

Previous speculation regarding cell activity within porous scaffolds has indicated that there exist an optimal, or range of optimal, pore size for each distinct cell type. This study produced a series of scaffolds with variable pore sizes and variable specific surface areas

available for cell attachment; this study showed a linear relationship between cell attachment and specific surface area, indicating that over the range of pore sizes studied (95.9 – 150.5 μm) short-term MC3T3 cell viability is governed by the specific surface area available for binding. The increasing cell viability with decreasing pore size would not be expected to continue as pore size would eventually drop to the point where cells could no longer fit into the pores. Future experiments, utilizing uniform scaffolds with a wider range or pore sizes and a wide variety of cell types would allow closer examination of factors other than specific surface area and their effects on cell viability. The results of this study, however, do help to explain the upper bound in biological activity observed for CG scaffolds used for *in vivo* tissue regeneration experiments that with increasing average pore diameter[1, 2]. In these studies, an upper limit in pore size was found for scaffolds used to induce regeneration where bioactive scaffolds were observed to induce binding of myofibroblasts (contractile cells) to the scaffold structure. At a sufficiently high pore diameter, the ligand density, directly proportional to the specific surface, becomes sufficiently small to support binding of only a small fraction of the contractile cells at the injured site. The data in this study support, therefore, the early hypothesis[2, 3] that the drop in scaffold activity with increasing pore diameter reflects a critical loss in ligand density.

Acknowledgments: We are grateful for the funding for this study provided by the Cambridge-MIT Institute (FJO, BAH, IVY, LJG) and the Fulbright Program (FJO), and to the Edelmann Laboratory in MIT for use of their facilities during histological

preparation of samples. Partial support (IVY) from an NIH/NIBIB Grant 8 R01 EB 000235 is also acknowledged.

FIGURE CAPTIONS

Figure 1. Average temperature of the freeze-dryer shelf (Fig. 1a) and the CG suspension (Fig. 1b) during freezing for the four constant-cooling rate freezing protocols.

Figure 2. Effect of freeze-drying temperature on mean pore size of CG scaffolds. One-way analysis of variance (ANOVA) showed that freezing temperature has a significant effect on the mean pore diameter ($p < 0.001$) of collagen-GAG scaffolds produced using this freeze-drying technique.

Figure 3. A series of micrographs taken of CG scaffolds fabricated at (Fig. 3a) -10ºC, (Fig. 3b) -20ºC, (Fig. 3c) -30ºC, and (Fig. 3d) -40ºC. Scaffolds fabricated at a lower final temperature of freezing have a smaller mean pore size. Scale bar = 100 μm.

Figure 4. Percentage of cells attached to the collagen-GAG scaffolds at 24 and 48 hours post seeding. One-way analysis of variance (ANOVA) showed that mean pore diameter of the scaffolds had a significant effect on cell attachment in both the 24 hour ($p < 0.01$) and 48 hour ($p < 0.001$) groups, and paired t-tests indicated that there was no significant difference in cell attachment between 24 and 48 hours for each scaffold ($p > 0.05$).

Figure 5. Attached cell number plotted against specific surface area showing a strong linear relationship at 24 hours (solid line) and 48 hours post seeding (solid line).

REFERENCES

1. Yannas, I.V., et al., *Synthesis and characterization of a model extracellular matrix that induces partial regeneration of adult mammalian skin.* Proc. Natl. Acad. Sci. USA, 1989. **86**(3): p. 933-937.
2. Yannas, I.V., *Tissue and Organ Regeneration in Adults*. 2001, New York: Springer.
3. Yannas, I.V., *Models of organ regeneration processes induced by templates*, in *Bioartificial Organs*, A. Prokop, D. Hunkeler, and A.D. Cherrington, Editors. 1997, Ann. N.Y. Acad. Sci. p. 280-293.
4. Luan, X. and T.G.H. Diekwisch, *CP27 affects viability, proliferation, attachment and gene expression in embryonic fibroblasts.* Cell Prolif., 2002. **35**(4): p. 207-219.
5. Howe, A., et al., *Integrin signaling and cell growth control.* Curr. Opin. Cell. Biol., 1998. **10**(2): p. 220-231.
6. Assoian, R.K. and X. Zhu, *Cell anchorage and the cytoskeleton as partners in growth factor dependent cell cycle progression.* Curr. Opin. Cell. Biol., 1997. **9**(1): p. 93-98.
7. Wake, M.C., C.W. Patrick, Jr., and A.G. Mikos, *Pore morphology effects on the fibrovascular tissue growth in porous polymer substrates.* Cell Transplant., 1994. **3**(4): p. 339-343.
8. van Tienen, T.G., et al., *Tissue ingrowth and degradation of two biodegradable porous polymers with different porosities and pore sizes.* Biomaterials, 2002. **23**(8): p. 1731-1738.
9. Chvapil, M., *Collagen sponge: theory and practice of medical applications.* J. Biomed. Mater. Res., 1977. **11**(5): p. 721-741.
10. Doillon, C.J., et al., *Collagen-based wound dressings: control of the pore structure and morphology.* J. Biomed. Mater. Res., 1986. **20**(8): p. 1219-1228.
11. Tsuruga, E., et al., *Pore size of porous hydroxyapatite as the cell-substratum controls BMP-induced osteogenesis.* J. Biochem., 1996. **2**: p. 317-324.
12. Zeltinger, J., et al., *Effect of pore size and void fraction on cellular adhesion, proliferation, and matrix deposition.* Tissue Eng., 2001. **7**(5): p. 557-572.
13. Salem, A.K., et al., *Interactions of 3T3 fibroblasts and endothelial cells with defined pore features.* J. Biomed. Mater. Res., 2002. **61**(2): p. 212-217.
14. Claase, M.B., et al., *Porous PEOT/PBT scaffolds for bone tissue engineering: preparation, characterization, and in vitro bone marrow cell culturing.* J. Biomed. Mater. Res., 2003. **64A**(2): p. 291-300.
15. Borden, M., et al., *Structural and human cellular assessment of a novel microsphere-based tissue engineered scaffold for bone repair.* Biomaterials, 2003. **24**(4): p. 597-609.
16. LiVecchi, A.B., R.M. Tombes, and M. LaBerge, *In vitro chondrocyte collagen deposition within porous HDPE: substrate microstructure and wettability effects.* J. Biomed. Mater. Res., 1994. **28**(8): p. 839-850.
17. Nehrer, S., et al., *Matrix collagen type and pore size influence behavior of seeded canine chondrocytes.* Biomaterials, 1997. **18**(11): p. 769-776.
18. Kuberka, M., et al., *Magnification of the pore size in biodegradable collagen sponges.* Int. J. Artif. Organs, 2002. **25**(1): p. 67-73.
19. Freyman, T.M., et al., *Fibroblast contraction of a collagen-GAG matrix.* Biomaterials, 2001. **22**(21): p. 2883-2891.
20. Freyman, T.M., I.V. Yannas, and L.J. Gibson, *Cellular materials as porous scaffolds for tissue engineering.* Prog. Mat. Sci., 2001. **46**: p. 273-282.
21. Hobbs, P.V., *Ice Physics*. 1974, Oxford: Clarendon Press.
22. Kurz, W. and D.J. Fisher, *Fundamentals of Solidification*. 1989, Switzerland: Transtech Publications.
23. Chang, A.S., et al., *Electrophysiological study of recovery of peripheral nerves regenerated by a collagen-glycosaminoglycan copolymer matrix*, in *Progress in Biomedical Polymers*, C.G. Gebelin and R.L. Dunn, Editors. 1990, Plenum Press: New York. p. 107-119.
24. Chang, A.S. and I.V. Yannas, *Peripheral Nerve Regeneration*, in *Encyclopedia of Neuroscience*, B. Smith and G. Adelman, Editors. 1992, Birkhauser: Boston. p. 125-126.
25. O'Brien, F.J., et al., *Influence of freezing rate on pore structure in freeze-dried collagen-GAG scaffolds.* Biomaterials, Submitted.

26. Kodama, H., et al., *Establishment of a clonal osteogenic cell line from newborn mouse calvaria.* Jpn. J. Oral Biol., 1981. **23**: p. 899-901.
27. Loree, H.M., et al. *A freeze-drying process for fabrication of polymeric bridges for peripheral nerve regeneration*. in *Proc. 15th Annual Northeast Bioeng. Conf.* 1989.
28. Michel, B., *Ice Mechanics*. 1978, Quebec: Les Presses De L'Universite Laval.
29. Yannas, I.V., *Collagen and gelatin in the solid state.* Rev. Macromol. Chem., 1972: p. 49B-104B.
30. Gibson, L.J. and M.F. Ashby, *Cellular Solids: Structure and Properties*, in *Cambridge Solid State Science Series*, D.R. Clarke, S. Suresh, and I.M. Ward, Editors. 1997, Cambridge University Press: Cambridge, U.K.
31. Williams, R.E., *Space-filling polyhedron: its relation to agregates of soap bubbles, plant cells and metal crystallites.* Science, 1968. **161**: p. 276-277.
32. Thompson, W., *On the division of space with minimum partition energy.* Phil. Mag., 1887. **24**: p. 503.
33. Kraynik, A.M., D.A. Reinelt, and F. van Swol, *Structure of random monodisperse foam.* Phys. Rev., 2003. **67**: p. 031403.
34. *Handbook of Chemistry and Physics*. 52 ed, ed. R.C. Weast. 1972, Cleveland, OH: Chemical Rubber Co.

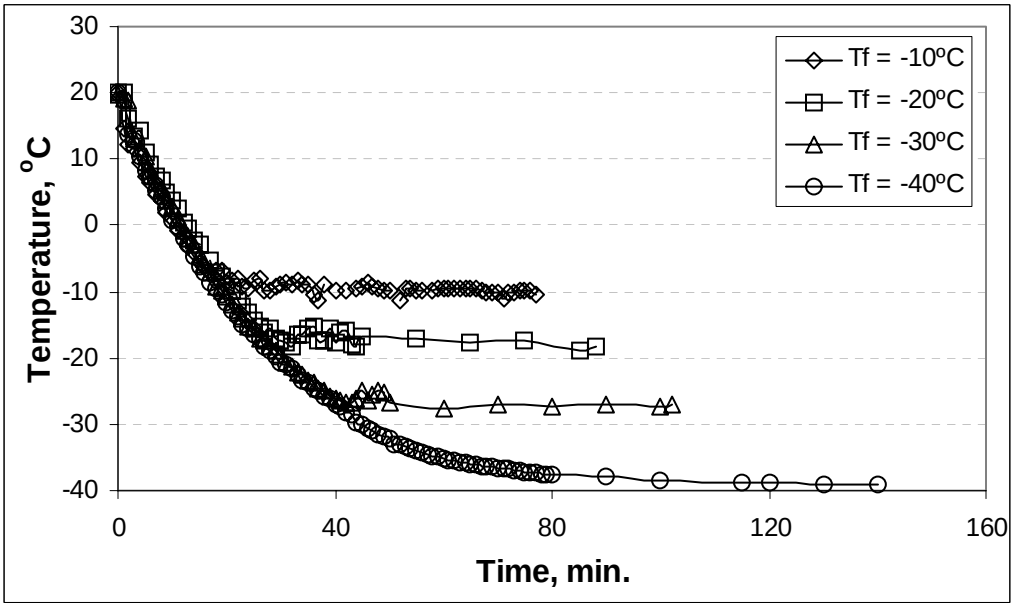

Fig. 1a

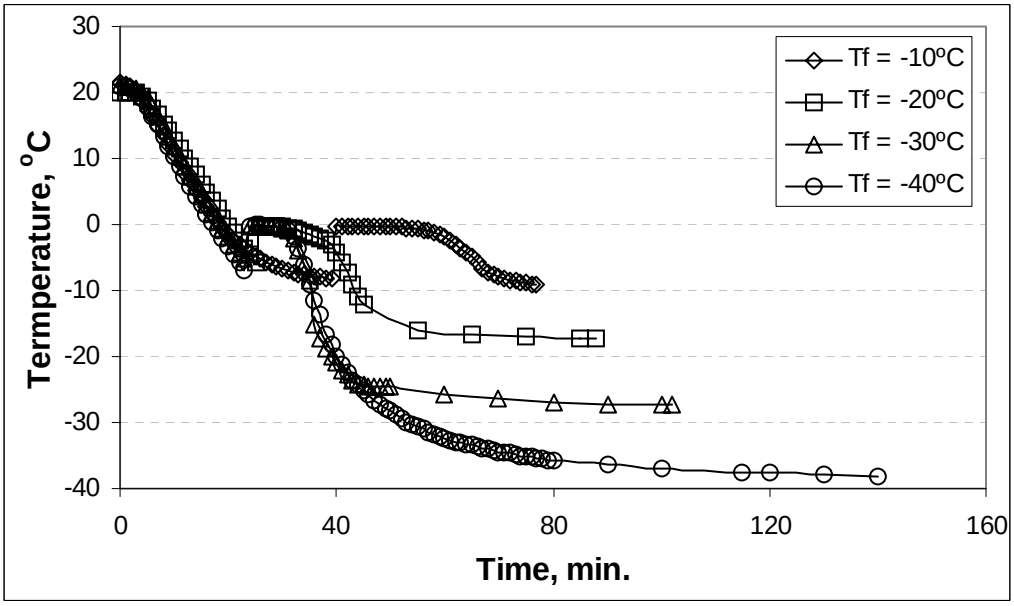

Fig. 1b

Figure 1. Average temperature of the freeze-dryer shelf (Fig. 1a) and the CG suspension (Fig. 1b) during freezing for the four constant-cooling rate freezing protocols.

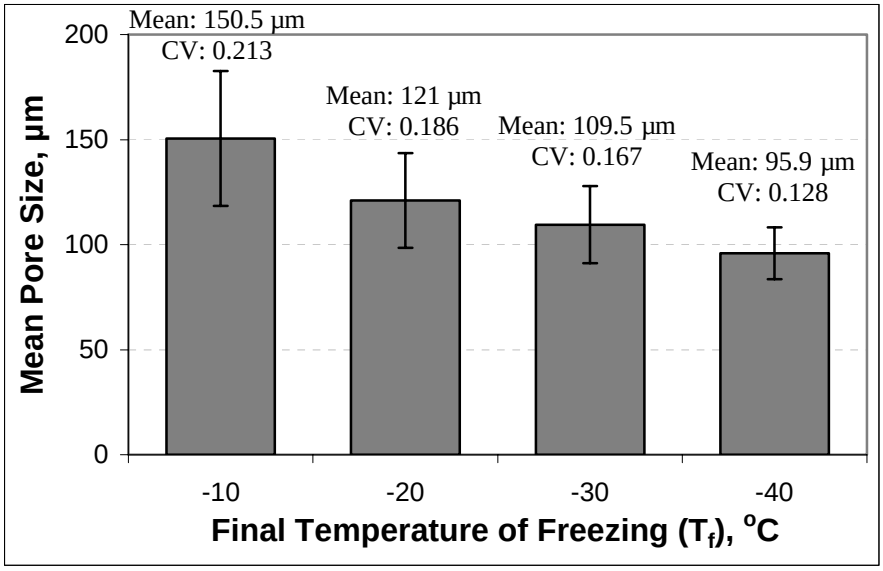

Figure 2. Effect of freeze-drying temperature on mean pore size of CG scaffolds. One-way analysis of variance (ANOVA) showed that freezing temperature has a significant effect on the mean pore diameter ($p < 0.001$) of collagen-GAG scaffolds produced using this freeze-drying technique.

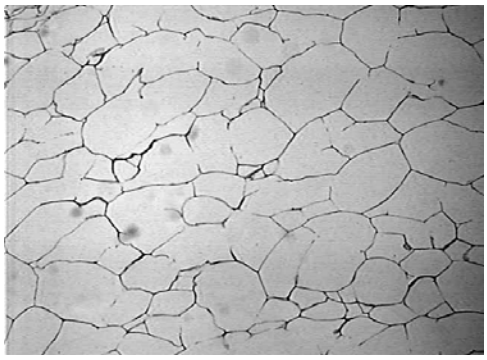

Fig. 3a

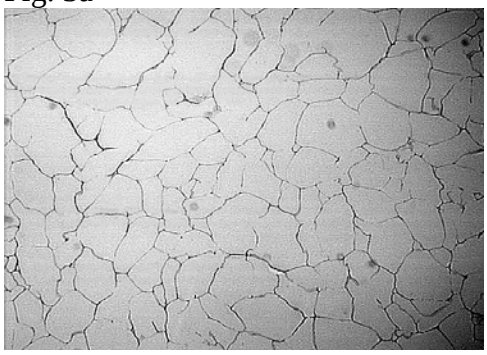

Fig. 3b

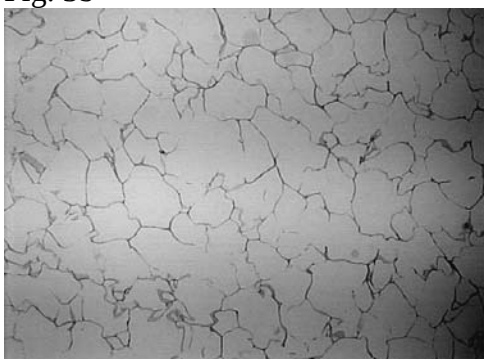

Fig. 3c

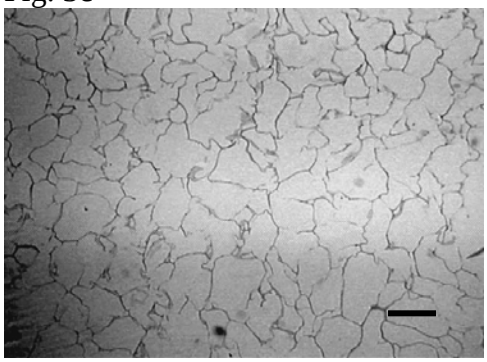

Fig. 3d

Figure 3. A series of micrographs taken of CG scaffolds fabricated at (Fig. 3a) -10ºC, (Fig. 3b) -20ºC, (Fig. 3c) -30ºC, and (Fig. 3d) -40ºC. Scaffolds fabricated at a lower final temperature of freezing have a smaller mean pore size. Scale bar = 100 μm.

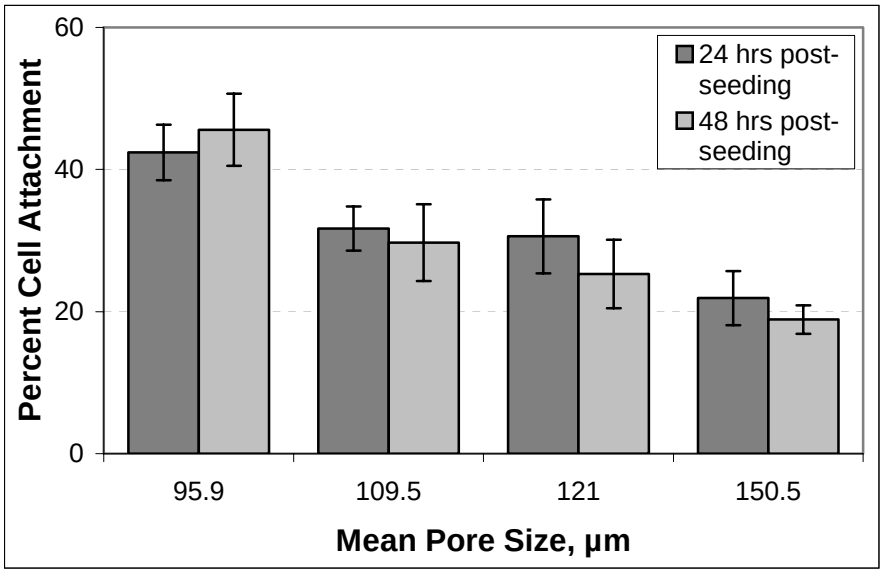

Figure 4. Percentage of cells attached to the collagen-GAG scaffolds at 24 and 48 hours post seeding. One-way analysis of variance (ANOVA) showed that mean pore diameter of the scaffolds had a significant effect on cell attachment in both the 24 hour ($p < 0.01$) and 48 hour ($p < 0.001$) groups, and paired t-tests indicated that there was no significant difference in cell attachment between 24 and 48 hours for each scaffold ($p > 0.05$).

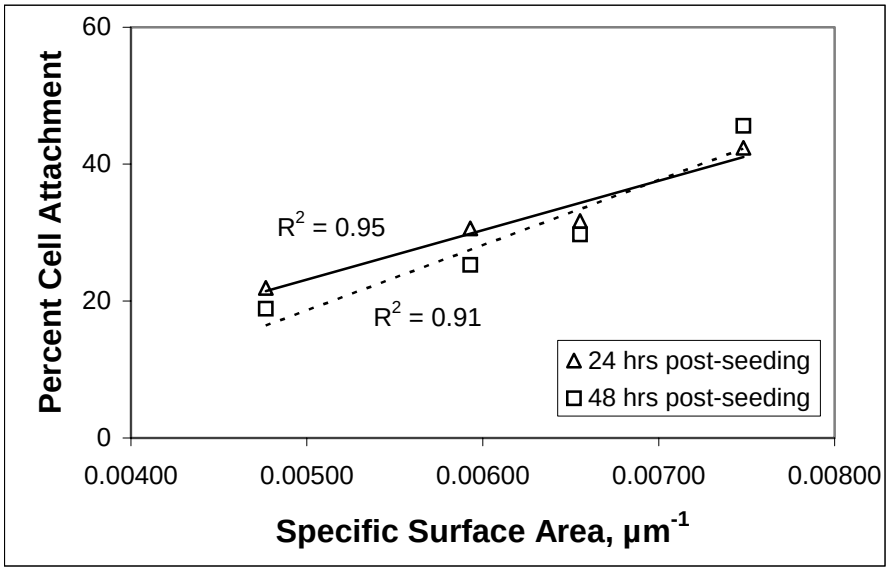

Figure 5. Attached cell number plotted against specific surface area showing a strong linear relationship at 24 hours (solid line) and 48 hours post seeding (dashed line).